

Charmonium-nucleon interaction from lattice QCD with a relativistic heavy quark action

Taichi Kawanai*

Department of Physics, The University of Tokyo, Hongo 7-3-1, Tokyo 113-0033, Japan
E-mail: kawanai@phys.s.u-tokyo.ac.jp

Shoichi Sasaki†

Department of Physics, The University of Tokyo, Hongo 7-3-1, Tokyo 113-0033, Japan
E-mail: ssasaki@phys.s.u-tokyo.ac.jp

Detailed information of the low-energy interaction between the charmonia (η_c and J/ψ) and the nucleon is indispensable for exploring the formation of charmonium bound to nuclei. In order to investigate the charmonium-nucleon interactions at low energies, we adopt two essentially different approaches in lattice QCD simulations. The charmonium-nucleon potential can be calculated from the equal-time Bethe-Salpeter amplitude through the effective Schrödinger equation. This novel method is based on the same idea originally applied for the nucleon force by Aoki-Hatsuda-Ishii. Another approach is to utilize extended Lüscher's formula with partially twisted boundary conditions, which allows us to calculate the s -wave phase shift at any small value of the relative momentum even in a finite box. We then extract model independent information of the scattering length and the effective range from the phase shift through the effective-range expansion. Our simulations are carried out at a lattice cutoff of $1/a \approx 2$ GeV in a spatial volume of $(3 \text{ fm})^3$ with the non-perturbatively $O(a)$ -improved Wilson fermions for the light quarks and a relativistic heavy quark action for the charm quark. Although our main results are calculated in quenched lattice calculations, we also present a preliminary full QCD result by using the 2+1 flavor gauge configurations generated by PACS-CS Collaboration. We have found that the charmonium-nucleon potential is weakly attractive at short distances and exponentially screened at large distances. We have also successfully evaluated both the scattering length and effective range from the charmonium-nucleon scattering phase shift.

The XXVIII International Symposium on Lattice Field Theory
June 14-19, 2010
Villasimius, Sardinia Italy

*Speaker for Charmonium-nucleon potential from lattice QCD.

†Speaker for Low energy charmonium-nucleon scattering with twisted boundary conditions.

1. Introduction

In past several years, properties of hadronic interactions have been extensively studied in lattice QCD simulations [1] based on Lüscher's finite size method, which is proposed as a general method for computing low-energy scattering phases of two particles in finite volume [2]. Here, we recall the recent great success of the nucleon-nucleon potential from lattice QCD [3]. In this new attempt, the "potential" between hadrons can be calculated from the equal-time Bethe-Salpeter (BS) amplitude through an effective Schrödinger equation [4]. A direct measurement of *hadron-hadron potentials* is now feasible by using lattice QCD. We also notice that an idea of partially twisted boundary conditions, which allows us to access any small value of non-zero momentum even in a finite volume, is quite useful for studying the hadron-hadron interaction at low energies through Lüscher's finite size method as originally proposed by Bedaque [5]. In this study, we exploit both novel approaches to obtain detailed information of the low-energy charmonium-nucleon interaction, that is essential for exploring the formation of charmonium bound to nuclei.

Heavy quarkonium states such as charmonium ($c\bar{c}$) states do not share the same quark flavor with the nucleon (N). This suggests that the heavy quarkonium-nucleon interaction is mainly induced by the genuine QCD effect of multi-gluon exchange [6, 7, 8]. Therefore the $c\bar{c}N$ system is ideal to study the effect of multi-gluon exchange between hadrons. As an analog of the van der Waals force, the simple two-gluon exchange contribution gives a weakly attractive, but long-ranged interaction [9, 10]. This implies that if such attraction between the charmonium and the nucleon is sufficiently strong, the charmonia (η_c and J/ψ) may be bound to the nucleon or to the large nuclei [6, 11]. In 1991, Brodsky *et al.* had argued that the $c\bar{c}$ -nucleus (A) bound state may be realized for the mass number $A \geq 3$, which Wasson confirmed later by solving the Schrödinger equation for the charmonium-nuclear system with the folding potential. Both calculations assumed a simple Yukawa form for the charmonium-nucleon potential as $V_{c\bar{c}N}(r) = -\gamma \exp(-\alpha r)/r$ where parameters ($\alpha = 0.6$ GeV, $\gamma = 0.6$) are fixed by a phenomenological Pomeron exchange model. However, the validity of calculations based on a phenomenological or perturbative theory is questionable for QCD where the strong interaction influences the long distance region.

The $c\bar{c}N$ scattering at low energy has been studied from first principles of QCD. The s -wave J/ψ - N scattering length is about 0.1 fm by using QCD sum rules [12] and 0.71 ± 0.48 fm (0.70 ± 0.66 fm for η_c - N) by lattice QCD [13], while it is estimated as large as 0.25 fm from the gluonic van der Waals interaction [7]. All studies suggest that the $c\bar{c}N$ interaction is weakly attractive. This indicates that the formation of charmonium bound to nuclei is enhanced. In this situation, precise information on the low energy charmonium-nucleon interaction is indispensable for exploring nuclear-bound charmonium states like the η_c - ^3He or J/ψ - ^3He bound state in few body calculations [14]. It should be quite important to give a firm theoretical prediction about the nuclear-bound charmonium, which is possibly investigated by experiments at J-PARC and FAIR/GSI.

2. Methodology

Let us briefly review two novel approaches employed in this study. First, we follow the recent

great success of the N - N potential from lattice QCD [3]. The potential between hadrons are calculated from the equal-time BS amplitude through an effective Schrödinger equation [3]. Second, we exploit partially twisted boundary conditions to calculate the scattering phase shift at low energies based on Lüscher's finite size method.

2.1 Hadron-hadron potential defined through the BS wave function

The method utilized here to calculate the hadron-hadron potential in lattice QCD is based on the same idea originally applied for the N - N potential [3, 4]. The first step in the derivation of the hadron-hadron potential is to define the BS wave function. We calculate the equal-time BS amplitude of two local operators (hadrons h_1 and h_2) separated by given spatial distances ($r = |\mathbf{r}|$) from the following four-point correlation function

$$G^{h_1-h_2}(\mathbf{r}, t; t_2, t_1) = \sum_{\mathbf{x}} \sum_{\mathbf{x}', \mathbf{y}'} \langle h_1(\mathbf{x}, t) h_2(\mathbf{x} + \mathbf{r}, t) (h_1(\mathbf{x}', t_2) h_2(\mathbf{y}', t_1))^\dagger \rangle, \quad (2.1)$$

where \mathbf{r} is the relative coordinate of two hadrons at sink position (t). Each hadron operator at source positions (t_1 and t_2) is separately projected onto a zero-momentum state by a summation over all spatial coordinates \mathbf{x}' and \mathbf{y}' . To avoid the Fierz rearrangement of two-hadron operators, it is better to set $t_2 \neq t_1$. Without loss of generality, we choose $t_2 = t_1 + 1 = t_{\text{src}}$ hereafter. Suppose that $|t - t_{\text{src}}| \gg 1$ is satisfied, the correlation function asymptotically behaves as

$$G^{h_1-h_2}(\mathbf{r}, t; t_{\text{src}}) \propto \phi_{h_1-h_2}(\mathbf{r}) e^{-E_{h_1-h_2}(t-t_{\text{src}})} \quad (2.2)$$

where the \mathbf{r} -dependent amplitude $\phi_{h_1-h_2}(\mathbf{r})$, which is defined by

$$\phi_{h_1-h_2}(\mathbf{r}) = \sum_{\mathbf{x}} \langle 0 | h_1(\mathbf{x}) h_2(\mathbf{x} + \mathbf{r}) | h_1 h_2; E_{h_1-h_2} \rangle, \quad (2.3)$$

with the total energy $E_{h_1-h_2}$ for the ground state of the two-particle h_1 - h_2 state, corresponds to a part of the equal-time BS amplitude and is called the BS wave function [2, 15]. After an appropriate projection with respect to discrete rotation

$$\phi_{h_1-h_2}^{A_1^+}(\mathbf{r}) = \frac{1}{24} \sum_{\mathcal{R} \in O_h} \phi_{h_1-h_2}(\mathcal{R}^{-1} \mathbf{r}), \quad (2.4)$$

where \mathcal{R} represents 24 elements of the cubic group O_h , one can get the BS wave function projected in the A_1^+ representation, which corresponds to the s -wave in continuum theory at low energy.

The BS wave function defined in Eqs.(2.3)-(2.4) obeys an effective Schrödinger equation with non-local potential $U_{h_1-h_2}$:

$$\left(\frac{1}{2\mu} \nabla^2 + E \right) \phi_{h_1-h_2}^{A_1^+}(\mathbf{r}) = \int U_{h_1-h_2}(\mathbf{r}, \mathbf{r}') \phi_{h_1-h_2}^{A_1^+}(\mathbf{r}') d^3 r', \quad (2.5)$$

where μ and E are a reduced mass and an energy eigenvalue of the two hadron system, respectively. The non-local potential $U_{h_1-h_2}$ defined in Eq.(2.5) is supposed to be energy independent. As long as considering the low energy hadron-hadron scattering, where the relative velocity of hadrons is small, we can take only the leading term in the velocity expansion. At low energy, the non-local potential in Eq.(2.5) may become localized as $U_{h_1-h_2}(\mathbf{r}, \mathbf{r}') = \delta(\mathbf{r} - \mathbf{r}') V_{h_1-h_2}(\mathbf{r})$. As a results, the

hadron-hadron “effective” central potential is defined through the following stationary Schrödinger equation

$$V_{h_1-h_2}(\mathbf{r}) = \frac{1}{2\mu} \frac{\nabla^2 \phi_{h_1-h_2}^{A_1^+}(\mathbf{r})}{\phi_{h_1-h_2}^{A_1^+}(\mathbf{r})} + E. \quad (2.6)$$

Once the BS wave functions $\phi_{h_1-h_2}^{A_1^+}(\mathbf{r})$, the reduced mass μ and energy eigenvalue E are calculated in lattice simulations, we can obtain the hadron-hadron potential from Eq.(2.6). For the differential operator ∇^2 , the discrete Laplacian with nearest-neighbor points is used. Although the energy eigenvalue E is supposed to be the energy difference between the total energy of two hadrons ($E_{h_1-h_2}$) and the sum of the rest mass of individual hadrons ($M_{h_1} + M_{h_2}$), we instead determine E with the condition of $\lim_{r \rightarrow \infty} \{ \frac{1}{2\mu} \nabla^2 \phi_{h_1-h_2}^{A_1^+}(\mathbf{r}) / \phi_{h_1-h_2}^{A_1^+}(\mathbf{r}) + E \} = 0$ [15]. More details of this method can be found in Ref. [4].

2.2 Lüscher’s finite size method with partially twisted boundary conditions

Let us consider the two-particle system in the center-of-mass frame, where the total energy of two-particle states is given by

$$E_{h_1-h_2}(p) = \sqrt{M_{h_1}^2 + p^2} + \sqrt{M_{h_2}^2 + p^2} \quad (2.7)$$

with the relative momentum $p = |\mathbf{p}|$. We here introduce the scaled relative momentum, $q = Lp/(2\pi)$, with the spatial extent L . Even under the periodic boundary condition, q^2 is no longer an integer due to the presence of two-particle interaction. In this sense, p is the interacting momentum. The s -wave phase shift $\delta_0(p)$ can be calculated through Lüscher’s phase-shift formula with the interacting momentum measured in the two-particle system:

$$p \cot \delta_0(p) = \frac{\mathcal{Z}_{00}(1, q^2)}{L\pi}, \quad (2.8)$$

where the generalized zeta function, $\mathcal{Z}_{00}(s, q^2) = \frac{1}{\sqrt{4\pi}} \sum_{\mathbf{n} \in \mathbf{Z}^3} (\mathbf{n}^2 - q^2)^{-s}$, is defined through an analytic continuation in s from the region $s > 3/2$ to $s = 1$ [2]. This is a general method for computing low-energy scattering phases of two particles in a finite box L^3 . As is well known, the quantity $p \cot \delta_0(p)$, which appears in the l.h.s. of Eq. (2.8), can be expanded in a power series of p^2 in the vicinity of the threshold as

$$p \cot \delta_0(p) = \frac{1}{a_0} + \frac{1}{2} r_0 p^2 + \mathcal{O}(p^4), \quad (2.9)$$

which is called the effective-range expansion [16]. It is worth noting that model-independent information of the low energy interaction should be encoded in a small set of parameters, *i.e.* the scattering length a_0 and the effective range r_0 , which are associated with the low energy constants in the effective field theory [17].

In principle, one can determine these threshold parameters through the detailed study of p^2 dependence of the scattering phase shift. However, it should be reminded that accessible values of the phase shift on the lattice are restricted due to the discrete momenta (approximately, in units of $2\pi/L$) in finite volume. Indeed, a typical size of the smallest non-zero momentum under the

periodic boundary condition, e.g. $p_{\min} \approx 2\pi/L \sim 420$ MeV for $L \simeq 3$ fm and 250 MeV for $L \simeq 5$ fm, which might be *beyond the radius of convergence for the effective-range expansion* at least in the attractive interaction case ¹.

A novel idea, twisted boundary condition, was proposed by Bedaque to circumvent the above mentioned issue [5]. If the following boundary conditions are imposed on quark fields $q(x)$ in a spatial direction ($i = 1, 2, 3$):

$$q(x_i + L) = e^{i\varphi_i} q(x), \quad (2.10)$$

where φ_i represents a twisted angle, all momenta in the spatial direction i are quantized in a finite box L^3 according to

$$p_i = \frac{2\pi}{L} \left(n_i + \frac{\varphi_i}{2\pi} \right), \quad (2.11)$$

where n_i becomes an integer in the free case. The case of $\varphi_i = 0$ (π) corresponds to the usual (anti-)periodic boundary condition. For non-zero twisted angle $\varphi_i \neq 0$, the lowest Fourier mode ($n_i = 0$) still can receive non-zero momentum φ_i/L , which can be set to an arbitrary small value. The redefinition of quark fields as $q'(x) = e^{i\vec{\theta} \cdot \vec{x}} q(x)$, where $\vec{\theta} = (\frac{\varphi_1}{L}, \frac{\varphi_2}{L}, \frac{\varphi_3}{L})$, can suggest how to implement the twisted boundary condition. The new fields $q'(x)$ now satisfy the usual periodic boundary conditions as $q'(x_i + L) = q'(x_i)$. Therefore, the hopping terms in the lattice fermion action are transformed [5] as

$$\sum_{i=1,2,3} \bar{q}'(x) \left[e^{ia\theta_i} U_i(x) (1 - \gamma_i) q'(x + \hat{i}) + e^{-ia\theta_i} U_i^\dagger(x - \hat{i}) (1 + \gamma_i) q'(x - \hat{i}) \right]. \quad (2.12)$$

This indicates that the quark propagator under the twisted boundary condition can be calculated with the simple replacement of the link variables $\{U_i(x)\}$ by $\{e^{ia\theta_i} U_i(x)\}$ in the hopping terms [5, 19]. The validity of this novel trick has been tested in the dispersion relation of single hadron states [19, 18]. It is also widely used for various purposes [20, 21, 22].

In this study, we apply twisted boundary conditions to two-hadron system in order to study properties of two-hadron scattering at low energies through Lüscher's finite size method as proposed in the original paper [5]. It should be reminded that the Lüscher's phase-shift formula receives a slight modification under twisted boundary conditions. The generalized zeta function $\mathcal{Z}_{00}(s, q^2)$ appeared in Eq. (2.8) should be replaced by the following function:

$$\mathcal{Z}_{00}^d(s, q^2) = \sum_{\mathbf{n} \in \mathbb{Z}^3} \frac{1}{((\mathbf{n} + \mathbf{d})^2 - q^2)^s} \quad (2.13)$$

with $\mathbf{d} = (\frac{\varphi_1}{2\pi}, \frac{\varphi_2}{2\pi}, \frac{\varphi_3}{2\pi})$ [5]. Although large L expansion formula is derived in Ref [5] as the asymptotic solution of the new phase-shift formula around the first pole of $q^2 = \mathbf{d}^2$, we instead use the extended Lüscher's phase-shift formula directly. For numerical evaluation of $\mathcal{Z}_{00}^d(1, q^2)$, we use a rapid convergent integral expression found in Appendix A of Ref. [23]. Within this approach, it is not necessary to calculate the higher Fourier modes of two-particle scattering state in order to examine the momentum dependence of the scattering phase shift near the threshold. It is known that different momentum modes in two-particle states do mix since the relative momentum is not conserved due to scattering [24]. In this sense, there is another advantage of this approach.

¹For the N - N scattering case, the convergence radius of is known to be smaller than $M_\pi/2$.

Table 1: Simulation parameters employed in this study.

n_f	β	$(\kappa_{\text{sea}}^{ud}, \kappa_{\text{sea}}^s)$	a^{-1} [GeV]	$L^3 \times T$	La [fm]	Stat.	M_π [GeV]
0	6.0	—	2.12	$32^3 \times 48$	2.98	602	0.64-0.87
2+1	1.9	(0.13754, 0.13640)	2.18	$32^3 \times 64$	2.90	450	0.41

3. Numerical results

We have performed lattice QCD simulations in both quenched and full QCD. In quenched QCD, we use a lattice size of $L^3 \times T = 32^3 \times 48$ with the single plaquette gauge action at $\beta = 6/g^2 = 6.0$, which corresponds to a lattice cutoff of $a^{-1} \approx 2.1$ GeV according to the Sommer scale [25, 26]. We use the non-perturbatively $\mathcal{O}(a)$ improved Wilson fermions for the light quarks (q) [27] and a relativistic heavy quark (RHQ) action for the charm quark (Q) [28]. The RHQ action is a variant of the Fermilab approach [29], which can remove large discretization errors for heavy quarks. The hopping parameter is chosen to be $\kappa_q = 0.1342, 0.1339, 0.1333$, which correspond to $M_\pi = 0.64, 0.72, 0.87$ GeV ($M_N = 1.43, 1.52, 1.70$ GeV), and $\kappa_Q = 0.1019$ which is reserved for the charm-quark mass ($M_{\eta_c} = 2.92$ GeV and $M_{J/\psi} = 3.00$ GeV) [30].

Full QCD simulations are also carried out by using 2+1 flavor gauge configurations generated by PACS-CS Collaboration on lattices of size $32^3 \times 64$ with the Iwasaki gauge action at $\beta = 1.9$, which corresponds to a comparable lattice cutoff of $a^{-1} \approx 2.2$ GeV, and the non-perturbatively $\mathcal{O}(a)$ improved Wilson fermions with $c_{SW} = 1.715$ [31]. Although we will present preliminary full QCD results for the η_c - N potential calculated at the third lightest quark mass ($\kappa_q = \kappa_{\text{sea}}^{ud} = 0.13754$) of the PACS-CS configurations [31], which corresponds to $M_\pi = 0.41$ GeV ($M_N = 1.20$ GeV), with $\kappa_Q = 0.10679$ for the charm quark ($M_{\eta_c} = 2.99$ GeV and $M_{J/\psi} = 3.10$ GeV), our main results are obtained from quenched lattice QCD. The simulation parameters and the number of sampled gauge configurations are summarized in Table 1.

We use the conventional interpolating operators, $h_1(x) = \epsilon_{abc}(u_a(x)C\gamma_5 d_b(x))u_c(x)$ for the nucleon, and $h_2(y) = \bar{c}_a(y)\gamma_5 c_a(y)$ for the η_c state or $h_2(y) = \bar{c}_a(y)\gamma_i c_a(y)$ for the J/ψ state, where a, b and c are color indices, and $C = \gamma_4\gamma_2$ is the charge conjugation matrix. Each hadron mass is obtained by fitting the corresponding two-point correlation function with a single exponential form. We calculate quark propagators with wall sources, which are located at $t_{\text{src}} = 5$ for the light quarks and at $t_{\text{src}} = 4$ for the charm quark, with Coulomb gauge fixing. It is worth mentioning that Dirichlet boundary conditions are imposed for quarks in the time direction in order to avoid wrap-around effects which are very cumbersome in systems of more than two hadrons [32]. In addition, the ground state dominance in four-point functions is checked by an effective mass plot of total energies of the $c\bar{c}$ - N system.

3.1 BS wave function and effective central potential

In this subsection, we mainly show results of the η_c - N interaction, which does not possess a spin-dependent part (see Ref. [33] for results of the J/ψ - N system). The left panel of Fig. 1 shows a typical result of the projected BS wave function at the smallest quark mass in quenched lattice QCD, which is evaluated by a weighted average of data in the time-slice range of $16 \leq t - t_{\text{src}} \leq 35$.

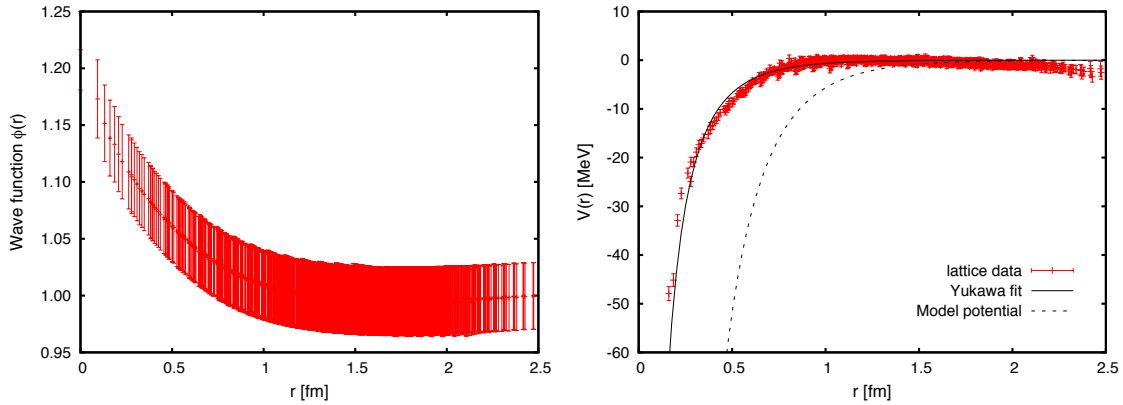


Figure 1: The BS wave function (left) and the effective central potential (right) in the s -wave η_c - N system for $M_\pi = 0.64$ GeV as a typical example. In the right panel we fit a Yukawa potential (solid line) and compare with the phenomenological potential (dashed) adopted in Ref. [6].

The wave functions are normalized to unity at a reference point $\mathbf{r} = (16, 16, 16)$, which is supposed to be outside of the interaction region. As shown in Fig. 1, the wave function is enhanced from unity near the origin so that the low-energy η_c - N interaction is certainly attractive. This attractive interaction, however, is not strong enough to form a bound state as is evident from this figure, where the wave function is not localized, but extends to large distances.

In the right panel of Fig. 1, we show the effective central η_c - N potential, which is evaluated by the wave function through Eq. (2.6) with measured values of E and μ . As is expected, the η_c - N potential clearly exhibits an entirely attractive interaction between the charmonium and the nucleon without any repulsion at either short or large distances. The short range attraction is deemed to be a result of the absence of Pauli blocking, that is a relevant feature in this particular system of the heavy quarkonium and the light hadron. The interaction is exponentially screened in the long distance region $r \gtrsim 1$ fm. This is consistent with the expected behavior of the color van der Waals force in QCD, where the strong confining nature of color electric fields must emerge [10, 34]. The exponential-type damping in the color van der Waals force is hardly introduced by any perturbative arguments.

In detail, a long-range screening of the color van der Waals force is confirmed by the following analysis. We have tried to fit data with two types of fitting functions: i) exponential type functions $-\exp(-r^m)/r^n$, which include the Yukawa form ($m = 1$ and $n = 1$), and ii) inverse power law functions $-1/r^m$, where n and m are not restricted to be integers. The former case can easily accommodate a good fit with a small χ^2/ndf value, while in the latter case we cannot get any reasonable fit. For example, the functional forms $-\exp(-r)/r$ and $-1/r^7$ give $\chi^2/\text{ndf} \simeq 2.5$ and 34.3, respectively. It is clear that the long range force induced by a normal “van der Waals” type interaction based on two-gluon exchange [10] is non-perturbatively screened.

If we adopt the Yukawa form $-\gamma e^{-\alpha r}/r$ to fit our data of $V_{c\bar{c}-N}(r)$, we obtain $\gamma \sim 0.1$ and $\alpha \sim 0.6$ GeV. These values should be compared with the phenomenological $c\bar{c}$ - N potential adopted in Refs. [6], where the parameters ($\gamma = 0.6$, $\alpha = 0.6$ GeV) are barely fixed by a Pomeron exchange model. The strength of the Yukawa potential γ is six times smaller than the phenomenological

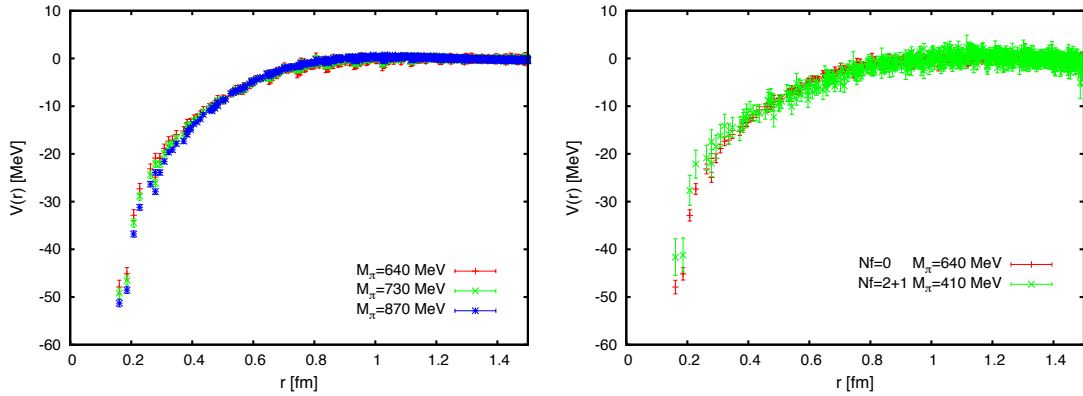


Figure 2: The quark-mass dependence of the η_c - N potential (left) and a comparison between quenched and dynamical simulations (right)

value, while the Yukawa screening parameter α obtained from our data is comparable. The $c\bar{c}$ - N potential derived from lattice QCD is rather weak.

We next show the quark-mass dependence of the η_c - N potential. As shown in the left panel of Fig. 2, large quark-mass dependence is not observed. This is a non-trivial feature since there is an explicit dependence on the reduced mass μ in the definition of the effective central potential Eq.(2.6). However, if one recalls that the $c\bar{c}$ - N interaction is mainly governed by multi-gluon exchange, the resulting potential is expected to be less sensitive to the reduced mass of the considered system ignoring the internal structures of the η_c and nucleon states.

In order to make a reliable prediction about the nuclear-bound charmonium, an important step is clearly an extension to dynamical lattice QCD simulations in the lighter quark mass region. Our preliminary result of the η_c - N potential at $M_\pi = 0.41$ GeV from 2+1 flavor dynamical QCD simulation is shown in the right panel of Fig. 2 where the η_c - N potential calculated at $M = 0.61$ GeV in quenched lattice QCD is also included for comparison. There is neither qualitative or quantitative differences between the quenched QCD result and the 2+1 flavor QCD result within statistical errors. This indicates that the η_c - N potential is not strongly affected by dynamical quarks at least up to $M_\pi = 0.41$ GeV.

It is worth remembering that the ordinary van der Waals interaction is sensitive to the size of the charge distribution, which is associated with the dipole size. Larger dipole size yields stronger interaction. We may expect that the size of the nucleon becomes large as the light quark mass decreases. However, the very mild quark-mass dependence and no appreciable dynamical quark effect observed here do not accommodate this expectation properly.

Recent detailed studies of nucleon form factors tell us that the root mean-square (rms) radius of the nucleon, which is a typical size of the nucleon, shows rather mild quark-mass dependence and its value is much smaller than the experimental value up to $M_\pi \sim 0.3$ GeV (for example, see [35]). At the chiral limit in baryon chiral perturbation theory the rms radius is expected to diverge logarithmically [36]. This implies that the size of the nucleon increases drastically in the vicinity of the physical point. It may be phenomenologically regarded as the ‘‘pion-cloud’’ effect.

To confirm the possible effect of the nucleon size on the $c\bar{c}$ - N potential as described previously,

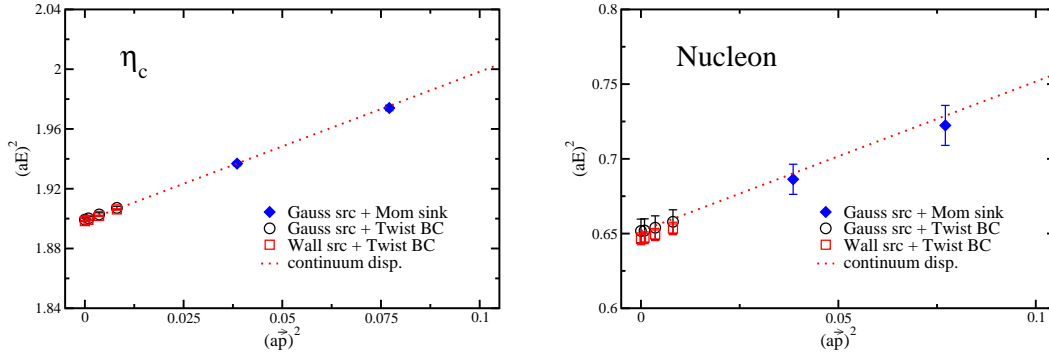


Figure 3: The square of measured energies of the η_c state (left) and the nucleon (right) as a function of three momentum squared in lattice unit. The dotted lines represents the relativistic and continuum-type dispersion relation.

we may need to perform simulations in much lighter quark mass region ($M_\pi < 0.3$ GeV). We speculate that the $c\bar{c}$ - N potential would become more attractive in the vicinity of the physical point where the “pion-cloud” effect emerges. Such planning is now underway [37].

3.2 Scattering under partially twisted boundary conditions

In this subsection, we present quenched QCD results of low-energy charmonium-nucleon scattering with partially twisted boundary conditions. The simulation set up is the same as what we use to calculate the η_c - N potential in quenched QCD. In this study, we introduce twisted boundary conditions only in a single direction, z -direction, where the D_4 point group symmetry still remains as a remnant of the rotation symmetry. Three non-zero twisted angles are chosen to be $\varphi_3 = \alpha, 2\alpha$ and 3α with $\alpha = 0.03 \times L \approx 3\pi/10$.

We first examine the dispersion relation of the charmonia (η_c and J/ψ) and the nucleon in order to demonstrate that finite momenta can be properly induced for the lowest Fourier mode ($|\mathbf{n}| = 0$) by the twisted angles. For comparing with results obtained from the higher Fourier modes ($|\mathbf{n}| \neq 0$) in the periodic boundary condition, we additionally calculate quark propagators with the gauge-invariant Gaussian smearing source [38]. We then compute two-point functions of the hadrons, where the sink hadron operators are projected onto the three lowest momenta, $(0, 0, 0)$, $(1, 0, 0)$ and $(1, 1, 0)$ in units of $2\pi/L$ in the periodic boundary condition (see details in Ref. [39]).

As shown in Fig. 3, we observe that measured energies of the η_c and the nucleon under partially twisted boundary conditions increases as twisted angles increase. Here, the momentum squared p^2 can be evaluated by $(\varphi_3/L)^2$. Data points of energies calculated by the standard technique of the momentum projection using the Fourier transformation are also included for comparison. All data points are consistent with the relativistic and continuum-type dispersion relation $E_h^2 = M_h^2 + p^2$. We recall that the dispersion relation is a key ingredient in determination of the relative momentum of two-particle states, which is required for Lüscher’s finite size method.

To determine the relative momentum of the charmonium-nucleon system, we consider the interaction energy E , which is defined by an energy difference between the total energy of two-

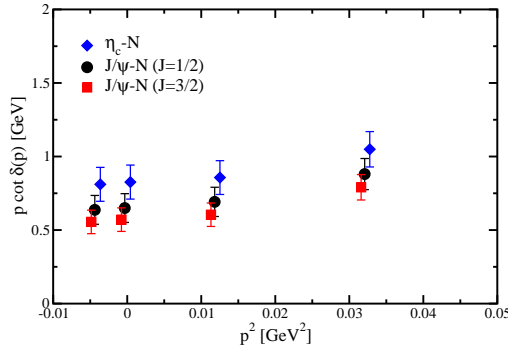


Figure 4: The value of $p \cot \delta_0(p)$ as a function of the interaction momentum squared p^2 at $M_\pi = 0.64$ GeV.

hadrons and the sum of the rest mass of individual hadrons:

$$E = E_{c\bar{c}N} - (M_{c\bar{c}} + M_N). \quad (3.1)$$

This energy value can be evaluated by the large- t behavior of a ratio of the four-point correlation function $G_{c\bar{c}N}(t) = \sum_{\mathbf{r}} G^{c\bar{c}N}(\mathbf{r}, t; t_{\text{src}})$ and two-point correlation functions of individual hadrons

$$R_{c\bar{c}N}(t) = \frac{G_{c\bar{c}N}(t)}{G_{c\bar{c}}(t)G_N(t)} \xrightarrow{t \gg t_{\text{src}}} \exp(-E(t - t_{\text{src}})) \quad (3.2)$$

where $G_{c\bar{c}}(t)$ and $G_N(t)$ represent two-point correlation functions of the charmonium and nucleon, respectively. The interacting momentum p , which is defined in Eq. (2.7), can be evaluated by this measured interaction energy E with the rest masses of individual hadrons, $M_{c\bar{c}}$ and M_N . Therefore, if the four-point function $G_{c\bar{c}N}(t)$ is calculated under the twisted boundary conditions, we can get various interacting momenta p near the threshold and also evaluate their corresponding scattering phase shifts through the extended Lüscher's phase shift formula, which is described in Sec. 2.2.

Fig. 4 shows the value of $p \cot \delta_0(p)$ calculated at the lightest quark mass ($M_\pi = 0.64$ GeV) as a function of the interaction momentum squared p^2 . Full diamond, circle and square symbols represent the η_c - N , spin-1/2 J/ψ - N and spin-3/2 J/ψ - N channels, respectively². All channels exhibit very mild momentum dependence near the threshold. Analyticity of $p \cot \delta_0(p)$ in the vicinity of the threshold allows us to consider the fit ansatz as a simple polynomial function of the interacting momentum squared p^2 :

$$p \cot \delta_0(p) = d_0 + d_1 p^2 + d_2 p^4. \quad (3.3)$$

Needless to say, it is nothing but the effective-range expansion. A linear fit with respect to p^2 for the three lowest p^2 points is enough to evaluate the first two fitting parameters, namely the scattering length $a_0 = 1/d_0$ and the effective range $r_0 = 2d_1$. We also apply a quadratic fit for all four data

²In the case of the s -wave J/ψ - N scattering, there are different spin states, spin-1/2 and 3/2 states. Therefore, the appropriate spin projections are required to disentangle each spin contribution from the four-point correlation functions. Details of the spin projection may be found in Appendix of Ref. [13].

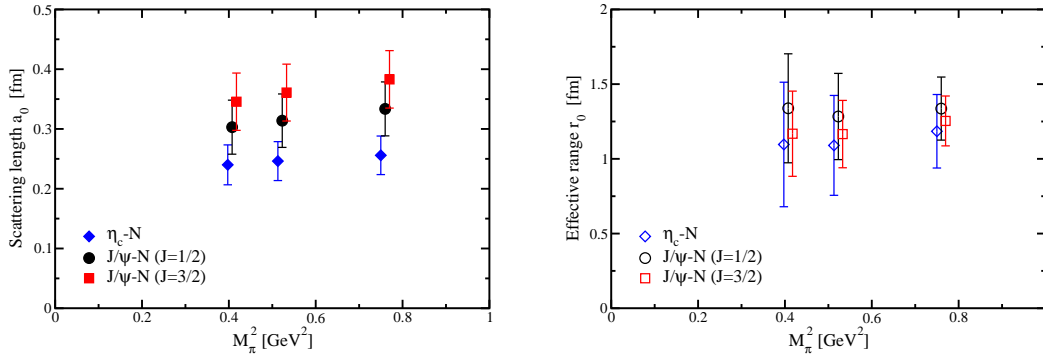


Figure 5: The scattering length a_0 (left) and effective range r_0 (right) as a function of M_π^2 . The squared (diamond) symbols have been moved slightly in the plus (minus) x-direction.

points. The scattering parameters obtained from both determinations agree with each other within their errors. We simply choose the values obtained from the linear fit as our final results.

In Fig. 5, we plot our evaluated scattering lengths (left panel) and effective ranges (right panel) for all three channels as a function of pion mass squared. In both scattering parameters, it is found that there is no significant quark mass dependence. These observations are consistent with what we observed in the charmonium-nucleon potentials. Although the channel dependence of the $c\bar{c}$ - N scattering length was less clear in previous studies [13, 40], we find $(a_0^{J/\psi-N})_{\text{SAV}} \sim 0.35 \text{ fm} > a_0^{\eta_c-N} \sim 0.25 \text{ fm}$ ³ in this study. On the other hand, both η_c - N and J/ψ - N channels yield the similar value of $r_0 \sim 1.0 \text{ fm}$ albeit with large errors. The former feature may indicate that the J/ψ - N system is slightly more attractive than the η_c - N system at low energy. This is consistent with the similar spin dependence observed in the difference of the η_c - N and J/ψ - N potentials [33].

4. Summary

We have studied low energy charmonium-nucleon interaction in both quenched and full QCD simulations. We first calculate potentials between the η_c state and the nucleon from the equal-time BS amplitude through the effective Schrödinger equation. We have found that the central potential $V_{c\bar{c}-N}(r)$ in the η_c - N system is weakly attractive at short distances and exponentially screened at large distances. It is observed that the potential have no significantly large quark-mass dependence within pion mass region $640 \text{ MeV} \leq M_\pi \leq 870 \text{ MeV}$ in quenched simulations. Our preliminary full QCD results show a good agreement with the quenched results. At least up to $M_\pi=410 \text{ MeV}$, we observe no appreciable dynamical quark effect on the charmonium-nucleon potential. We have also employed an alternative approach for studying the charmonium-nucleon interaction. The s -wave phase shifts at low energies are calculated through the extended Lüscher's finite size method with twisted boundary conditions. We have successfully evaluated both the scattering length and effective range from the charmonium-nucleon scattering phase shift in the vicinity of the threshold, where the effective range expansion is applicable. We have found $(a_0^{J/\psi-N})_{\text{SAV}} \sim 0.35 \text{ fm} > a_0^{\eta_c-N} \sim$

³Here SAV stands for the spin-averaged value $\frac{1}{3}[(a_0)_{1/2} + 2(a_0)_{3/2}]$ for the J/ψ - N channel.

0.25 fm, while all η_c - N and J/ψ - N channels yield the similar value of $r_0 \sim 1.0$ fm albeit with large errors. The channel dependence observed in the $c\bar{c}$ - N scattering length may indicate that the J/ψ - N system is slightly more attractive than the η_c - N system at low energy. This is fairly consistent with what we reported in Ref. [33], where the difference between the η_c - N and J/ψ - N potentials are discussed.

Acknowledgement

We would like to thank T. Hatsuda for helpful suggestions and fruitful discussions. We also thank PACS-CS Collaboration for their gauge configurations. T.K. is supported by Grant-in-Aid for JSPS Fellows (No. 22-7653). S.S. is supported by the JSPS Grant-in-Aids for Scientific Research (C) (No. 19540265) and Scientific Research on Innovative Areas (No. 21105504). Numerical calculations reported here were carried out on the PACS-CS supercomputer at CCS, University of Tsukuba and also on the T2K supercomputer at ITC, University of Tokyo.

References

- [1] See, e.g. S. R. Beane PoS **LATTICE2008**, 008 (2008) [arXiv:0812.1236 [hep-lat]] and references therein.
- [2] M. Lüscher, Nucl. Phys. B **354**, 531 (1991).
- [3] N. Ishii, S. Aoki and T. Hatsuda, Phys. Rev. Lett. **99**, 022001 (2007).
- [4] S. Aoki, T. Hatsuda and N. Ishii, Prog. Theor. Phys. **123** (2010) 89.
- [5] P. F. Bedaque, Phys. Lett. B **593**, 82 (2004).
- [6] S. J. Brodsky, I. A. Schmidt and G. F. de Teramond, Phys. Rev. Lett. **64**, 1011 (1990).
- [7] S. J. Brodsky and G. A. Miller, Phys. Lett. B **412**, 125 (1997).
- [8] M. E. Luke, A. V. Manohar and M. J. Savage, Phys. Lett. B **288**, 355 (1992).
- [9] T. Appelquist and W. Fischler, Phys. Lett. B **77**, 405 (1978).
- [10] G. Feinberg and J. Sucher, Phys. Rev. D **20**, 1717 (1979).
- [11] D. A. Wasson, Phys. Rev. Lett. **67**, 2237 (1991).
- [12] A. Hayashigaki, Prog. Theor. Phys. **101**, 923 (1999).
- [13] K. Yokokawa, S. Sasaki, T. Hatsuda and A. Hayashigaki, Phys. Rev. D **74**, 034504 (2006).
- [14] V. B. Belyaev et al., Nucl. Phys. A **780**, 100 (2006).
- [15] S. Aoki *et al.* [CP-PACS Collaboration], Phys. Rev. D **71**, 094504 (2005).
- [16] R. G. Newton, "Scattering Theory of Waves and Particles", 2nd ed. (Springer, New York, 1982).
- [17] P. F. Bedaque and U. van Kolck, Ann. Rev. Nucl. Part. Sci. **52**, 339 (2002).
- [18] G. M. de Divitiis, R. Petronzio and N. Tantalo, Phys. Lett. B **595**, 408 (2004).
- [19] J. M. Flynn, A. Juttner and C. T. Sachrajda [UKQCD Collaboration], Phys. Lett. B **632**, 313 (2006).
- [20] P. A. Boyle, J. M. Flynn, A. Juttner, C. T. Sachrajda and J. M. Zanotti, JHEP **0705**, 016 (2007).

- [21] P. A. Boyle *et al.*, JHEP **0807**, 112 (2008).
- [22] C. H. Kim and C. T. Sachrajda, Phys. Rev. D **81**, 114506 (2010).
- [23] T. Yamazaki *et al.* [CP-PACS Collaboration], Phys. Rev. D **70**, 074513 (2004).
- [24] L. Maiani and M. Testa, Phys. Lett. B **245** (1990) 585.
- [25] R. Sommer, Nucl. Phys. B **411**, 839 (1994).
- [26] M. Guagnelli, R. Sommer and H. Wittig [ALPHA collaboration], Nucl. Phys. B **535**, 389 (1998); S. Necco and R. Sommer, Nucl. Phys. B **622**, 328 (2002)
- [27] M. Lüscher, S. Sint, R. Sommer, P. Weisz and U. Wolff, Nucl. Phys. B **491**, 323 (1997).
- [28] S. Aoki, Y. Kuramashi and S. I. Tominaga, Prog. Theor. Phys. **109**, 383 (2003).
- [29] A. X. El-Khadra, A. S. Kronfeld and P. B. Mackenzie, Phys. Rev. D **55**, 3933 (1997).
- [30] Y. Kayaba *et al.* [CP-PACS Collaboration], JHEP **0702**, 019 (2007).
- [31] S. Aoki *et al.* [PACS-CS Collaboration], Phys. Rev. D **79**, 034503 (2009).
- [32] T. T. Takahashi, T. Umeda, T. Onogi and T. Kunihiro, Phys. Rev. D **71**, 114509 (2005).
- [33] T. Kawanai and S. Sasaki, Phys. Rev. D **82**, 091501(R) (2010).
- [34] S. Matsuyama and H. Miyazawa, Prog. Theor. Phys. **61**, 942 (1979).
- [35] T. Yamazaki *et al.*, Phys. Rev. D **79**, 114505 (2009).
- [36] M. A. B. Beg and A. Zepeda, Phys. Rev. D **6**, 2912 (1972).
- [37] T. Kawanai and S. Sasaki (in progress).
- [38] S. Gusken, Nucl. Phys. Proc. Suppl. **17** (1990) 361.
- [39] S. Sasaki and T. Yamazaki, Phys. Rev. D **78**, 014510 (2008).
- [40] L. Liu, H. W. Lin and K. Orginos, PoS LATTICE2008, 112 (2008) [arXiv:0810.5412 [hep-lat]].